

Sintering process as relevant parameter for Bi₂O₃ vaporization from ZnO-Bi₂O₃-based varistor ceramics

XU Dong(徐东)¹, CHENG Xiao-nong(程晓农)¹, YAN Xue-hua(严学华)¹,
XU Hong-xing(徐红星)¹, SHI Li-yi(施利毅)²

1. School of Materials Science and Engineering, Jiangsu University, Zhenjiang 212013, China;
2. School of Materials Science and Engineering, Shanghai University, Shanghai 200072, China

Received 10 August 2009; accepted 15 September 2009

Abstract: The relationship between sintering process and vaporization of the Bi₂O₃ in ZnO-Bi₂O₃-based varistor ceramics was investigated. The phase and microstructure evolution during the sintering process were examined. The results show that the higher the sintering temperature or the longer the sintering time is, the more the Bi₂O₃ is volatilized. The heating rate has little effects on the Bi₂O₃ volatilized in ZnO-Bi₂O₃-based varistor ceramics. This is in accordance with the relative X-ray diffraction peak area ratio analysis. The results also show that the sintering temperature has the greatest impact on the vaporization of the Bi₂O₃, then followed by sintering time, and the effect of the heating rate is the minimum.

Key words: varistor; ZnO; vaporization; sintering process; microstructure

1 Introduction

ZnO varistors show a highly nonlinear current–voltage characteristic with a highly resistive state in the prebreakdown region and large non-linearity coefficient[1–2]. Non-ohmic conduction in ZnO varistors is a grain-boundary phenomenon, which has often been explained by thermionic emission enhanced by barrier lowering at low fields with a combination of other mechanisms at high fields[3–4]. The method of sintering process is critical for producing good varistor materials. Commercial varistors are usually made by solid state of ZnO particles with doping agent oxides such as Bi₂O₃, Sb₂O₃, Co₂O₃, MnO₂ and Cr₂O₃, then the mixed powder is pressed and sintered at higher temperatures. A complex microstructure can be achieved, in which conducting ZnO grains, electrically insulating secondary spinel phase and Bi-rich inter-granular phase are found[5]. In other words, the microstructure of the ZnO varistors consists of highly conductive n-type ZnO grains and electrically insulating Schottky barriers of grain boundaries.

In the classical ZnO-based varistor, Bi₂O₃ is used as the varistor-former, thus it is essential for inducing the

nonlinearity of the ZnO varistors[6–7]. Bi₂O₃ is particularly important since it provides the medium for liquid-phase sintering, enhances the growth of ZnO grains, and affects the stability of the nonlinear current-voltage characteristics of the material. The melting point of Bi₂O₃ is 825 °C, and the eutectic temperature of ZnO-Bi₂O₃ is only 740 °C, thus a liquid is formed in the ZnO-Bi₂O₃ specimens below 800 °C. As soon as the eutectic liquid is formed, the mass loss starts to increase. This indicates that the vaporization of Bi₂O₃ starts immediately after the eutectic liquid has been formed[8].

RUBIA et al[9–10] used the X-ray fluorescence method to investigate the effect of the area-to-volume ratio on the vaporization of Bi in ZnO varistors. To reduce the loss of material, METZ et al[8] suggested using a new route, in which ceramics are produced by mixing pre-synthesized spinel and pyrochlore phases with other classical single-oxide additives. ONREABROY et al[11] have noted that the nonlinearity coefficient depended primarily on the sintering temperature, which significantly decreased at higher temperatures, probably due to the volatilization of Bi₂O₃. Mass loss by uncontrolled Bi₂O₃ vaporization is a crucial parameter in the manufacture of varistor ceramics[12].

XU et al[4] investigated the effect of sintering method, such as open sintering, sintering inside a closed crucible, and sintering within a powder bed, on the vaporization of the Bi_2O_3 in ZnO- Bi_2O_3 -based varistor ceramics. By using a sufficient amount of powder bed, the mass loss of Bi_2O_3 reduces from $>95\%$ to $<20\%$ [13]. However, the effects of the different sintering processes on the vaporization of the Bi_2O_3 in varistor ceramics have seldom been reported.

In this work, attention is given to the relationship between sintering process and vaporization of the Bi_2O_3 in varistor ceramics. The phase and microstructure evolution during the sintering process are also investigated.

2 Experimental

Reagent-grade raw materials were used in proportions of 96.5% ZnO, 0.7% Bi_2O_3 , 1.0% Sb_2O_3 , 0.8% Co_2O_3 , 0.5% Cr_2O_3 and 0.5% MnO_2 (molar fraction). After milling, the mixture was dried at $70\text{ }^\circ\text{C}$ for 24 h, then the power was uniaxially pressed into discs of 12 mm in diameter and 2 mm in thickness. The pressed discs were sintered with three different sintering processes. First, some of the pressed discs were sintered at five fixed sintering temperature of 900, 1 000, 1 100, 1 200, and 1 300 $^\circ\text{C}$ in air for 2 h, labeled as FA1, FA2, FA3, FA4 and FA5, respectively, using a heating rate of $5\text{ }^\circ\text{C}/\text{min}$ and then cooled in the furnace. Second, some of the pressed discs were sintered in air at 1 100 $^\circ\text{C}$ for 2 h, using a heating rate of 1, 2, 5 and 10 $^\circ\text{C}/\text{min}$, and then all of the samples were cooled in the furnace, labeled as FB1, FB2, FB3 and FB4, respectively. Finally, the others of the pressed discs were sintered in air at 1 100 $^\circ\text{C}$ for 0 h, 0.5 h, 1 h, 2 h, 4 h and 6 h, labeled as FC1, FC2, FC3, FC4, FC5 and FC6, respectively, using a heating rate of $5\text{ }^\circ\text{C}/\text{min}$ and then cooled in the furnace. The sintered samples were all lapped and polished to 1.0 mm in thickness. The final samples were about 10 mm in diameter and 1.0 mm in thickness.

The bulk density of the samples was measured in terms of their mass and volume. For the characterization of DC current and voltage, the silver paste was coated on both faces of samples and the silver electrodes were formed by heating at $600\text{ }^\circ\text{C}$ for 10 min. The electrodes were 5 mm in diameter. The voltage—current ($V-I$) characteristics were measured using a $V-I$ source/measurement unit (CJP CJ1001). The nominal varistor voltages (V_N) at 0.1 mA and 1 mA were measured and the threshold voltage V_T (V/mm) ($V_T=V_N(\text{at } 1\text{ mA})/d$, where d is the thickness of the sample, mm) and nonlinear coefficient α ($\alpha=1/\lg[V_N(\text{at } 1\text{ mA})/V_N(\text{at } 0.1$

mA)]) were determined. The leakage current (I_L) was measured at $0.75V_N$ (at 1 mA). The crystalline phases were identified by an X-ray diffractometer (XRD, Rigaku D/max 2200, Japan) using a Cu K_α radiation. The surface microstructure was examined by a scanning electron microscope (SEM, FEI QUANTA 400). The Bi-concentration of sintered bodies was analyzed using an inductively coupled plasma atomic emission spectrometer (ICP-AES; Plasma-400).

3 Results and discussion

Fig.1 shows the XRD patterns of varistor ceramics sintered at different sintering temperatures for 2 h with $5\text{ }^\circ\text{C}/\text{min}$ heating rate. The samples consist typically of three phases: ZnO, spinel and Bi-rich phase. The XRD peak intensities of the spinel phase and the intergranular Bi-rich phase change with the sintering temperature. No Bi_2O_3 can be detected in the specimens sintered at 1 300 $^\circ\text{C}$. Bi_2O_3 can be found in the samples sintered at 900–1 300 $^\circ\text{C}$, and the higher the sintering temperature is, the weaker the XRD peak intensities of Bi_2O_3 are. Table 1 presents the effect of the sintering temperature on the relative X-ray diffraction peak area ratio, which indicates the different phase amount in the varistor ceramics, such as ZnO, spinel and Bi-rich phase. As can be seen from Table 1, the higher the sintering temperature is, the less the amount of Bi_2O_3 is, which also shows that the higher the sintering temperature is, the more the Bi_2O_3 is volatilized. This result is in accordance with the ICP analysis. From ICP, the vaporization losses of the Bi_2O_3 in the samples FA1, FA2, FA3, FA4 and FA5 are 10.9%, 11.5%, 31.4%, 75.3%, and 94.6%, respectively.

Fig.2 shows the SEM images of varistor ceramics sintered at different sintering temperatures for 2 h with

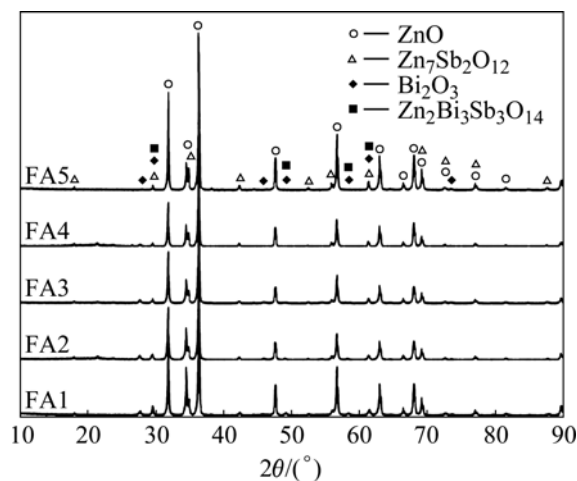
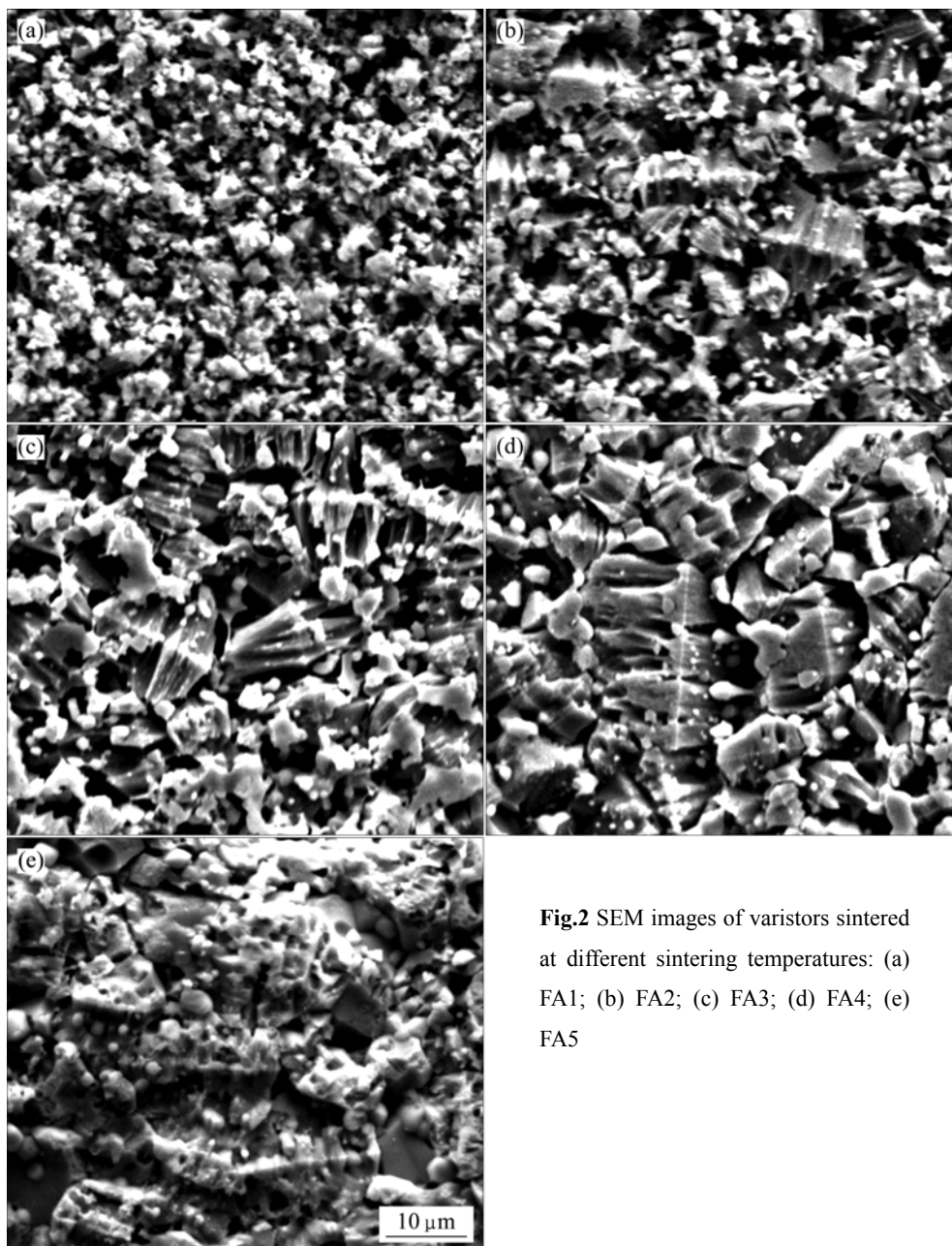


Fig.1 XRD patterns of varistors sintered at different temperatures

Table 1 Effect of sintering temperature on relative X-ray diffraction peak area ratio

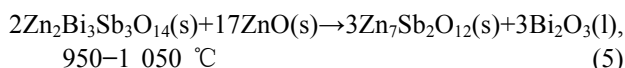
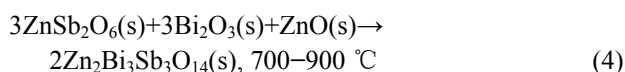
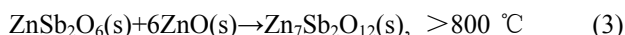
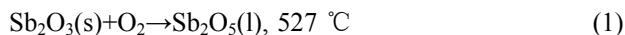
Sample	$\text{Bi}_2\text{O}_3(310)/\text{ZnO}(101)$	$\text{Zn}_2\text{Bi}_3\text{Sb}_3\text{O}_{14}(222)/\text{ZnO}(101)$	$\text{Zn}_7\text{Sb}_2\text{O}_{14}(311)/\text{ZnO}(101)$
FA1	0.047	0.079	0.388
FA2	0.047	0.073	0.258
FA3	0.040	0.047	0.237
FA4	0.025	0.034	0.190
FA5	–	0.024	0.217

**Fig.2** SEM images of varistors sintered at different sintering temperatures: (a) FA1; (b) FA2; (c) FA3; (d) FA4; (e) FA5

5 °C/min heating rate. A similar microstructure of the samples is obtained in all cases with some differences coming from the average size of ZnO grains[14–15] due to the different sintering temperatures. Meanwhile, with increasing the sintering temperature, the differences of inter-granular phase in SEM become more and more

obvious.

Differential thermal and high temperature X-ray analysis have recently suggested the following reactions for the microstructure development of ZnO varistor during reactive liquid phase sintering in the temperature range of 500–1 050 °C [8, 16]:



According to reactions (1)–(4), at the first stage of sintering, after the formation of spinel (ZnSb_2O_6 , $\text{Zn}_7\text{Sb}_2\text{O}_{12}$) and pyrochlore ($\text{Zn}_2\text{Bi}_3\text{Sb}_3\text{O}_{14}$) phases, pyrochlore reacts with ZnO to lead to the appearance of a liquid bismuth oxide phase by reaction (5), and the formation of spinel is accompanied with the formation of Bi_2O_3 liquid simultaneously. In other words, this liquid oxide might dissolve adjacent to solid ZnO phases, generating an eutectic liquid rich in bismuth; and at the same time, the decrease of pyrochlore and the increase of spinel take place[8]. The generation of the Bi_2O_3 -rich liquid induces the formation of capillary forces, which brings the second phase together to form cluster (see Fig.2(c)). As soon as the Bi_2O_3 -rich liquid is formed, the vaporization starts. The mass loss of the varistor ceramics thus jumps as the temperature is raised above $1\text{ }000\text{ }^\circ\text{C}$, just as the vaporization loss of the Bi_2O_3 from 11.5% at $1\text{ }000\text{ }^\circ\text{C}$ to 31.4% at $1\text{ }100\text{ }^\circ\text{C}$, confirming that the reaction (5) takes place at a temperature around $1\text{ }000\text{ }^\circ\text{C}$ [7]. When the sintering temperature is $1\text{ }300\text{ }^\circ\text{C}$, the vaporization loss of the Bi_2O_3 is very serious[17], up to 94.6%, and the Bi-rich inter-granular phase almost disappears (see Fig.2(e)).

Fig.3 shows the XRD patterns of varistor ceramics sintered at $1\text{ }100\text{ }^\circ\text{C}$ for 2 h with different heating rates. The samples also consist typically of three phases: ZnO, spinel and intergranular Bi-rich phase. Bi_2O_3 can be detected in every sample sintered at $1\text{ }100\text{ }^\circ\text{C}$ for 2 h with different heating rates. Table 2 presents the effect of the heating rate on the relative X-ray diffraction peak area ratio, which indicates the different phase amount in the varistor ceramics, such as ZnO, spinel and Bi-rich phase. As can be seen from Table 2, regardless of the

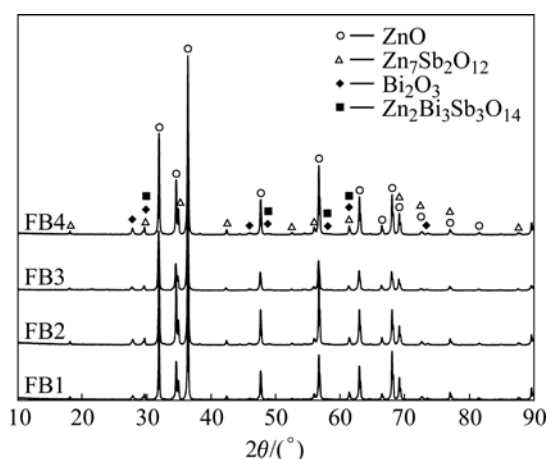


Fig.3 XRD patterns of varistor sintered with different heating rates

heating rate, the vaporization of the Bi_2O_3 in every example is very similar. From ICP one also knows the vaporization losses of the Bi_2O_3 in the samples FB1, FB2, FB3 and FB4 are 34.7%, 31.7%, 31.4% and 31.1%, respectively. Fig.4 shows the SEM images of varistor ceramics sintered at $1\text{ }100\text{ }^\circ\text{C}$ for 2 h with different heating rates. A similar microstructure of the samples is obtained in all cases with some differences coming from the average grain size. It is indicated the heating rate has little effect on the grain morphology of the varistor ceramics.

The sintering time has an important effect on the varistor ceramics[18–19]. Fig.5 shows the XRD patterns of varistor ceramics sintered at $1\text{ }100\text{ }^\circ\text{C}$ for different sintering time with $5\text{ }^\circ\text{C}/\text{min}$ heating rate. The samples consist typically of three phases: ZnO, spinel and intergranular Bi-rich phase. The XRD peak intensities of the spinel phase and the intergranular Bi-rich phase vary with the sintering time. Bi_2O_3 can be found in the samples sintered at $1\text{ }100\text{ }^\circ\text{C}$ for different sintering time, and the longer the sintering time is, the weaker the XRD peak intensities of Bi_2O_3 are. Table 3 presents the effect of the sintering time on the relative X-ray diffraction peak area ratio, which indicates the different phase amount in the varistor ceramics, such as ZnO, spinel and Bi-rich phase. As can be seen from Table 3, the longer the sintering time is, the less the amount of Bi_2O_3 is, and the more the Bi_2O_3 is volatilized. These results are in

Table 2 Effect of heating rate on relative X-ray diffraction peak area ratio

Sample	$\text{Bi}_2\text{O}_3(310)/\text{ZnO}(101)$	$\text{Zn}_2\text{Bi}_3\text{Sb}_3\text{O}_{14}(222)/\text{ZnO}(101)$	$\text{Zn}_7\text{Sb}_2\text{O}_{14}(311)/\text{ZnO}(101)$
FB1	0.045	0.045	0.338
FB2	0.048	0.053	0.380
FB3	0.040	0.047	0.237
FB4	0.049	0.051	0.337

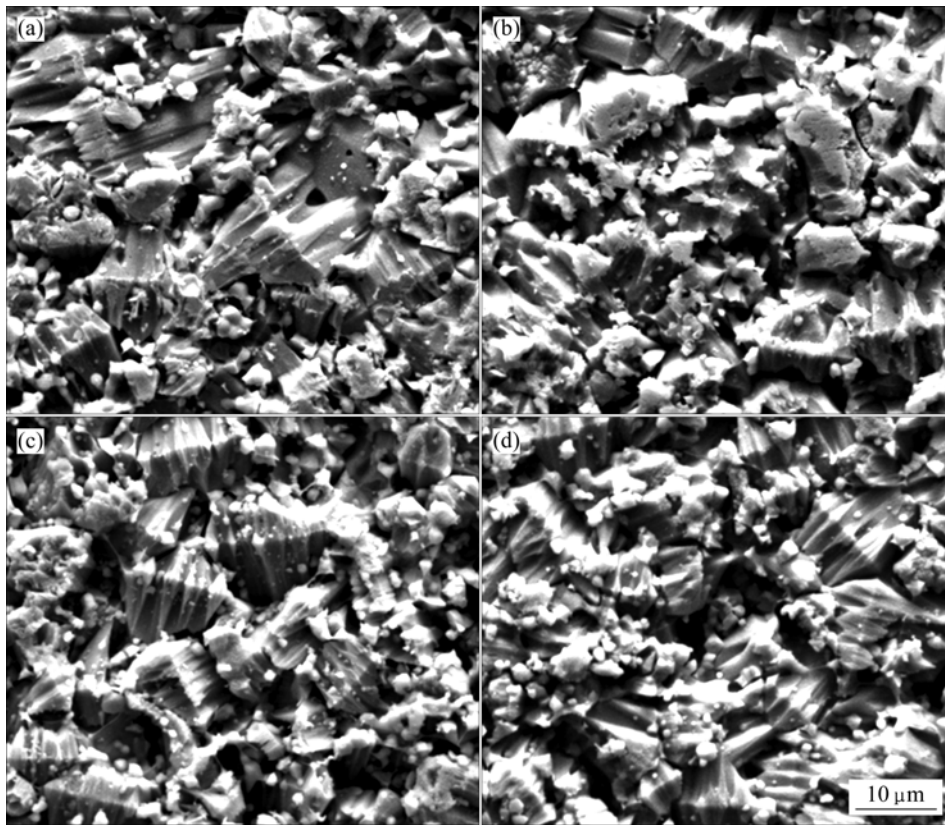


Fig.4 SEM images of varistor sintered with different heating rates: (a) FB1; (b) FB2; (c) FB3; (d) FB4

Table 3 Effect of sintering time on relative X-ray diffraction peak area ratio

Sample	$\text{Bi}_2\text{O}_3(310)/\text{ZnO}(101)$	$\text{Zn}_2\text{Bi}_3\text{Sb}_3\text{O}_{14}(222)/\text{ZnO}(101)$	$\text{Zn}_7\text{Sb}_2\text{O}_{14}(311)/\text{ZnO}(101)$
FC1	0.066	0.073	0.349
FC2	0.059	0.059	0.342
FC3	0.052	0.059	0.359
FC4	0.040	0.047	0.237
FC5	0.041	0.049	0.352
FC6	0.034	0.035	0.327

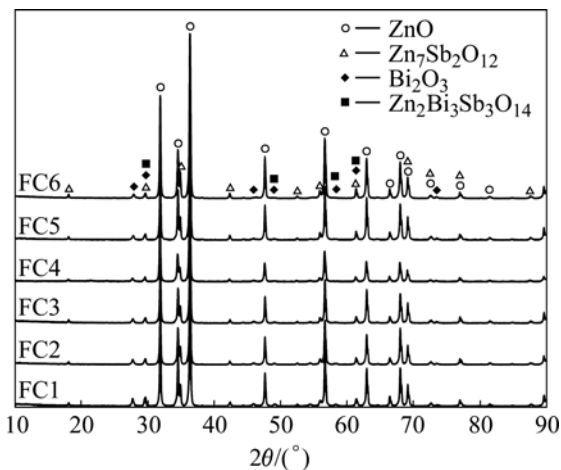


Fig.5 XRD patterns of varistor sintered with different sintering time

accordance with the ICP analysis. The ICP shows the vaporization losses of the Bi_2O_3 in the samples FC1, FC2, FC3, FC4, FC5 and FC6 are 5.2%, 21.0%, 26.4%, 31.4%, 40.0%, and 42.2%, respectively. The SEM images of varistor ceramics sintered at 1 100 °C for different sintering time with 5 °C/min heating rate are presented in Fig.6. It is observed that the longer the sintering time is, the bigger the grains grow. At the same time, the microstructures are still very similar, and the grain morphology only has a little change.

From the analyses of the SEM, XRD and ICP of the different sintering temperature, heating rate, holding time of the samples, we can see the sintering temperature has the greatest impact on the vaporization of the Bi_2O_3 , followed by sintering time, and the effect of the heating rate is the minimum.

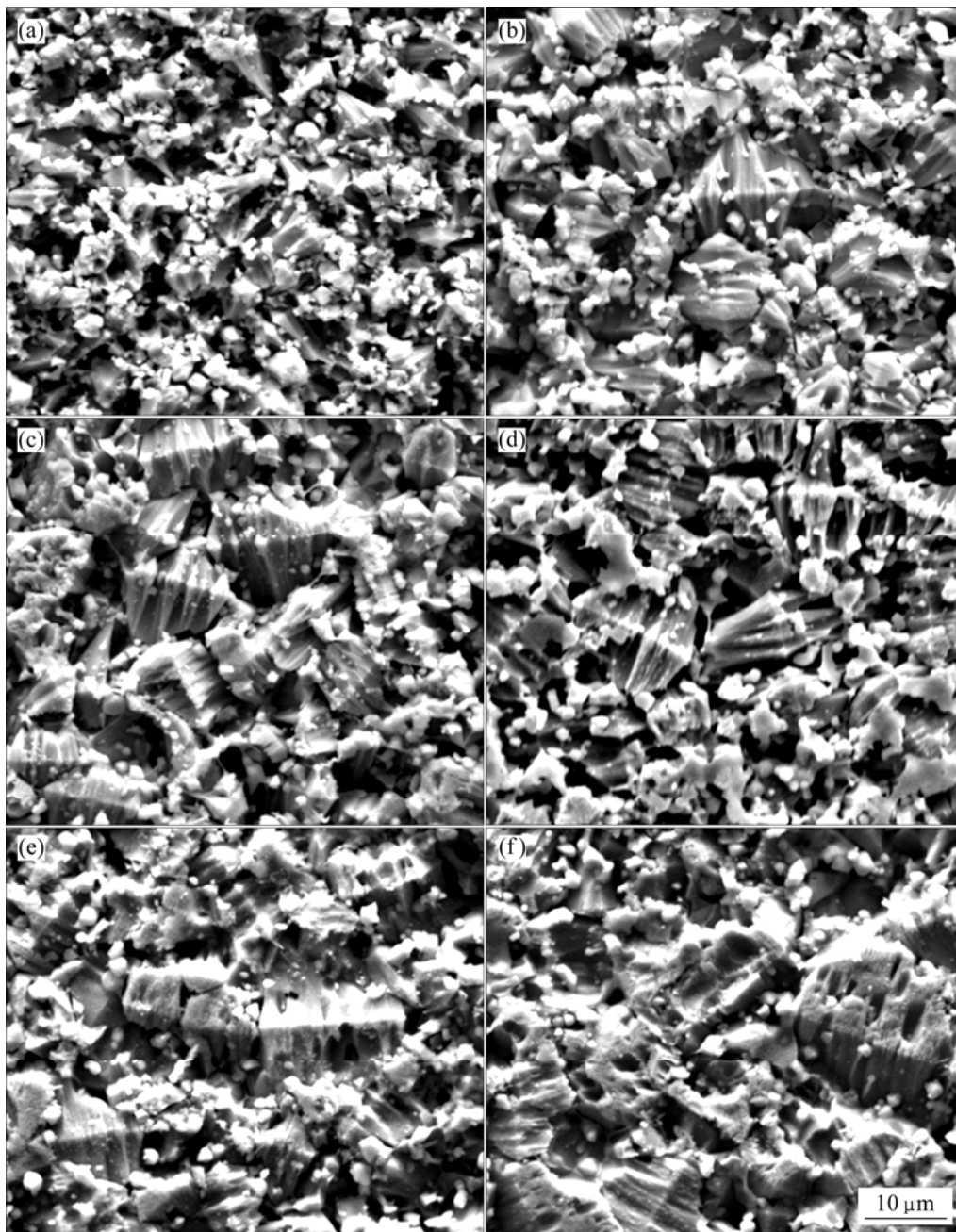


Fig.6 SEM images of varistor sintered with different sintering time: (a) FC1; (b) FC2; (c) FC3; (d) FC4; (e) FC5; (f) FC6

4 Conclusions

1) The higher the sintering temperature is or the longer the sintering time is, the more the Bi_2O_3 is volatilized.

2) The heating rate has little effects on the Bi_2O_3 volatilized in $\text{ZnO-Bi}_2\text{O}_3$ -based varistor ceramics.

3) The sintering temperature has the greatest impact on the vaporization of the Bi_2O_3 , then followed by sintering time, and the effect of the heating rate is the minimum.

References

- [1] CLARKE D R. Varistor ceramics [J]. *J Am Ceram Soc*, 1999, 82(3): 485–502.
- [2] ANAS S, MANGALARAJA R V, POOTHAYAL M, SHUKLA S K, ANANTHAKUMAR S. Direct synthesis of varistor-grade doped nanocrystalline ZnO and its densification through a step-sintering technique [J]. *Acta Mater*, 2007, 55(17): 5792–5801.
- [3] BUENO P R, VARELA J A, LONGO E. SnO_2 , ZnO and related polycrystalline compound semiconductors: An overview and review on the voltage-dependent resistance (non-ohmic) feature [J]. *J Eur Ceram Soc*, 2008, 28(3): 505–529.
- [4] XU D, SHI L, WU Z, ZHONG Q, WU X. Microstructure and electrical properties of $\text{ZnO-Bi}_2\text{O}_3$ -based varistor ceramics by

- different sintering processes [J]. *J Eur Ceram Soc*, 2009, 29(9): 1789–1794.
- [5] PILLAI S C, KELLY J M, MCCORMACK D E, O'BRIEN P, RAMESH R. The effect of processing conditions on varistors prepared from nanocrystalline ZnO [J]. *J Mater Chem*, 2003, 13(10): 2586–2590.
- [6] ELFWING M, OSTERLUND R, OLSSON E. Differences in wetting characteristics of Bi₂O₃ polymorphs in ZnO varistor materials [J]. *J Am Ceram Soc*, 2000, 83(9): 2311–2314.
- [7] LAO Y W, KUO S T, TUAN W H. Effect of Bi₂O₃ and Sb₂O₃ on the grain size distribution of ZnO [J]. *J Electroceram*, 2007, 19(2/3): 187–194.
- [8] METZ R, DELALU H, VIGNALOU J R, ACHARD N, ELKHATIB M. Electrical properties of varistors in relation to their true bismuth composition after sintering [J]. *Mater Chem Phys*, 2000, 63(2): 157–162.
- [9] de la RUBIA M A, PEITEADO M, FERNANDEZ J F, CABALLERO A C. Compact shape as a relevant parameter for sintering ZnO-Bi₂O₃ based varistors [J]. *J Eur Ceram Soc*, 2004, 24(6): 1209–1212.
- [10] PEITEADO M, de la RUBIA M A, VELASCO M J, VALLE F J, CABALLERO A C. Bi₂O₃ vaporization from ZnO-based varistors [J]. *J Eur Ceram Soc*, 2005, 25(9): 1675–1680.
- [11] ONREABROY W, SIRIKULRAT N, BROWN A P, HAMMOND C, MILNE S J. Properties and intergranular phase analysis of a ZnO-CoO-Bi₂O₃ varistor [J]. *Solid State Ionics*, 2006, 177(3/4): 411–420.
- [12] KIM C H, KIM J H. Microstructure and electrical properties of ZnO-ZrO₂-Bi₂O₃-M₃O₄ (M=Co, Mn) varistors [J]. *J Eur Ceram Soc*, 2004, 24(8): 2537–2546.
- [13] LAO Y W, KUO S T, TUAN W H. Effect of powder bed on the microstructure and electrical properties of Bi₂O₃- and Sb₂O₃-doped ZnO [J]. *J Mater Sci: Mater Electron*, 2009, 20(3): 234–241.
- [14] CAI J N, LIN Y H, LI M, NAN C W, HE J L, YUAN F L. Sintering temperature dependence of grain boundary resistivity in a rare-earth-doped ZnO varistor [J]. *J Am Ceram Soc*, 2007, 90(1): 291–294.
- [15] NAHM C W. Effect of sintering temperature electrical properties of ZNR doped with Pr-Co-Cr-La [J]. *Ceram Int*, 2008, 34(6): 1521–1525.
- [16] LEITE E R, NOBRE M A, LONGO E, VARELA J A. Microstructural development of ZnO varistor during reactive liquid phase sintering [J]. *J Mater Sci*, 1996, 31(20): 5391–5398.
- [17] LEACH C, VERNON-PARRY K. The effect of sintering temperature on the development of grain boundary traps in zinc oxide based varistors [J]. *J Mater Sci*, 2006, 41(12): 3815–3819.
- [18] SANTOS P A, MARUCHIN S, MENEGOTO G F, ZARA A J, PIANARO S A. The sintering time influence on the electrical and microstructural characteristics of SnO₂ varistor [J]. *Mater Lett*, 2006, 60(12): 1554–1557.
- [19] NAHM C W. Influence of sintering time on electrical and dielectric behavior, and DC accelerated aging characteristics of Dy³⁺-doped ZnO-Pr₆O₁₁-based varistors [J]. *Mater Chem Phys*, 2005, 94(2/3): 275–282.

(Edited by YANG Bing)